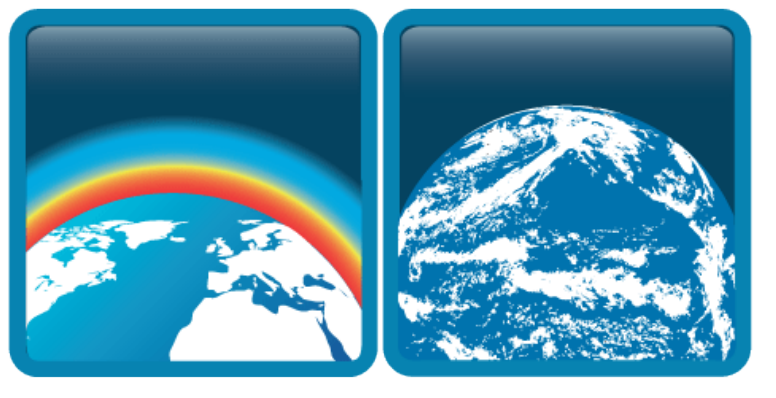


# Cloud-aerosol interactions downwind of localised aerosol sources

A.C. Povey<sup>1,2,\*</sup>, M.W. Christensen<sup>1</sup>, G.M. McGarragh<sup>1</sup>, C.A. Poulsen<sup>2,3</sup>,  
S.R. Proud<sup>1</sup>, G.E. Thomas<sup>3</sup>, R.G. Grainger<sup>1,2</sup>

<sup>1</sup>University of Oxford, UK; <sup>2</sup>NCEO, UK; <sup>3</sup>RAL Space, UK; \*adam.povey@physics.ox.ac.uk



## Introduction

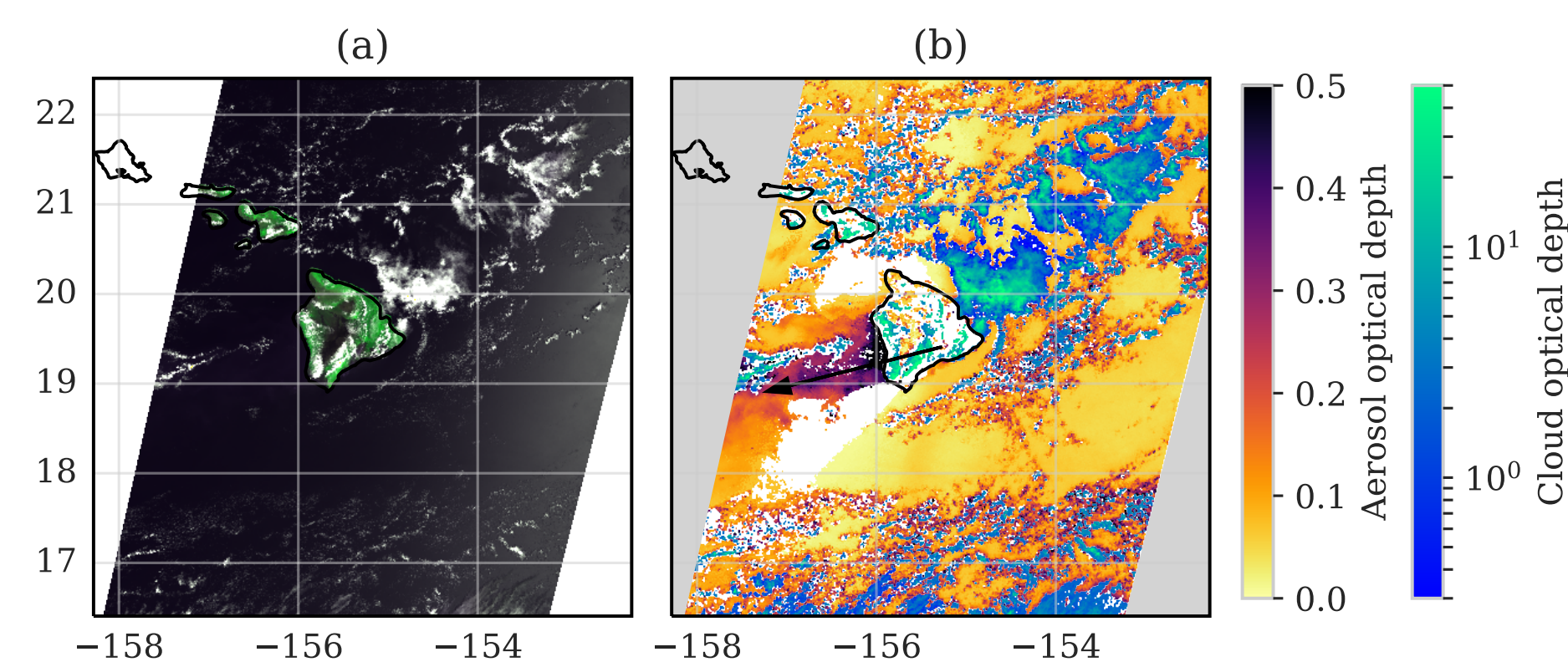
This poster outlines ongoing work to quantify the variation of cloud effective radius (CER) and cloud albedo (ALB) as a function of aerosol index (AI) by using localised aerosol sources, such as volcanoes, as a natural laboratory. Satellite retrievals by the Optimal Retrieval of Aerosol and Cloud (ORAC) are provided by the recently completed cloud and aerosol Climate Change Initiative (CCI) datasets, which can be downloaded from <http://cci.esa.int>. Further details on the datasets can be found in [1, 2].

ORAC [3, 4] is a generalised optimal estimation scheme [5] to retrieve cloud, aerosol, and surface properties from satellite-based visible and/or infrared measurements. It is open-source software developed by a world-wide community of researchers within a version control system managed by the British Atmospheric Data Group (BADC). The Fortran 90 source code can be obtained from <http://proj.badc.rl.ac.uk/orac> and processes observations from (A)ATSR, AVHRR, MODIS, and SEVIRI (with other sensors easily added) to retrieve:

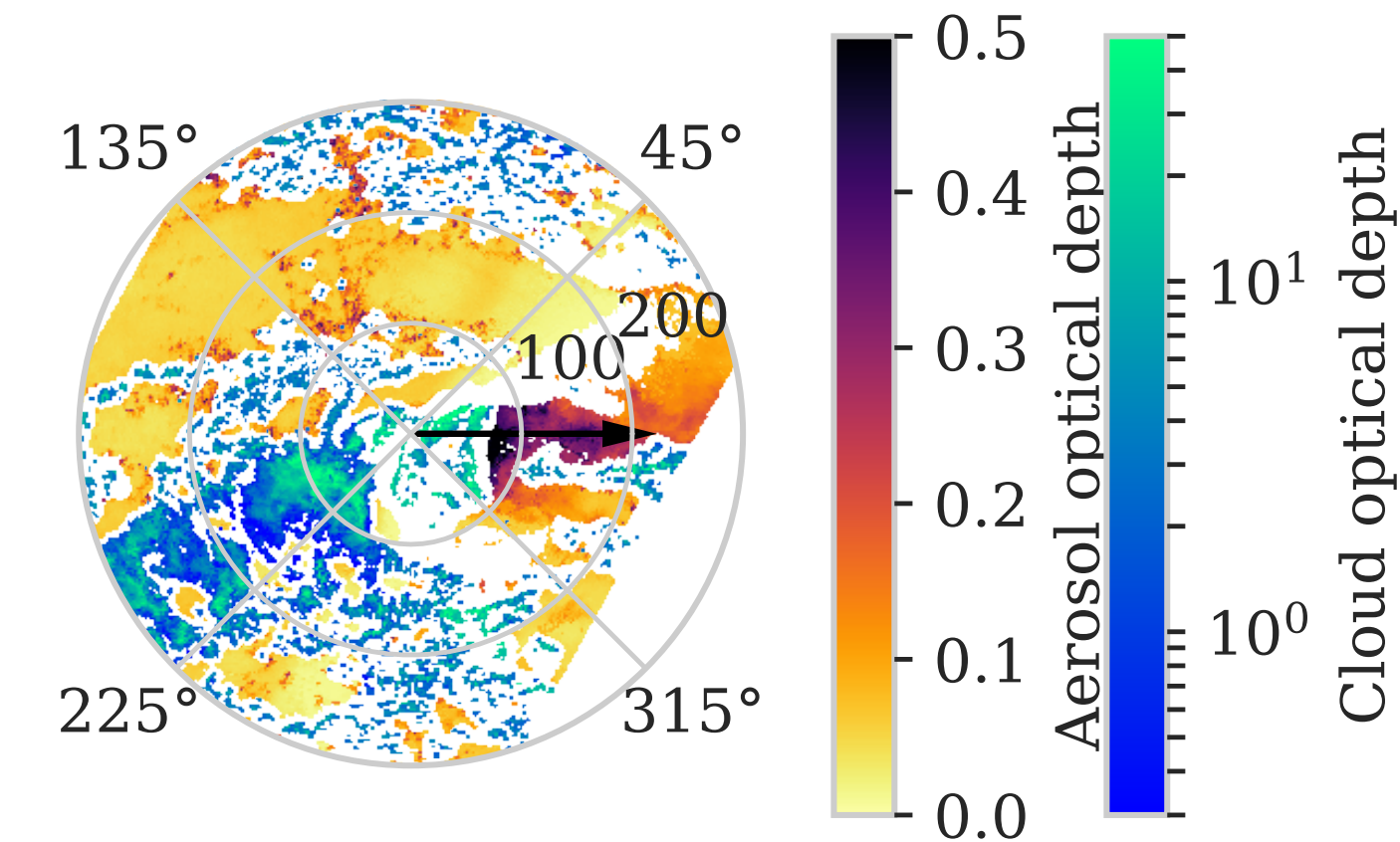
- aerosol optical thickness (AOT) and effective radius with surface reflectance (at 550 nm);
- aerosol optical thickness, effective radius, and layer height with sea surface temperature;
- cloud optical thickness (COT), effective radius, and top pressure with surface temperature; or
- volcanic ash optical thickness, effective radius, and plume top pressure.

## Localised aerosol sources

The example below shows (a) a false-colour image from AATSR over Hawaii on 9 Sep 2008 and (b) the ORAC retrieval from that image at 1 km resolution, with the wind vector shown by an arrow. A plume of aerosol is evident downwind due to passive degassing from Mt. Kilauea and is intermingled with cloud.

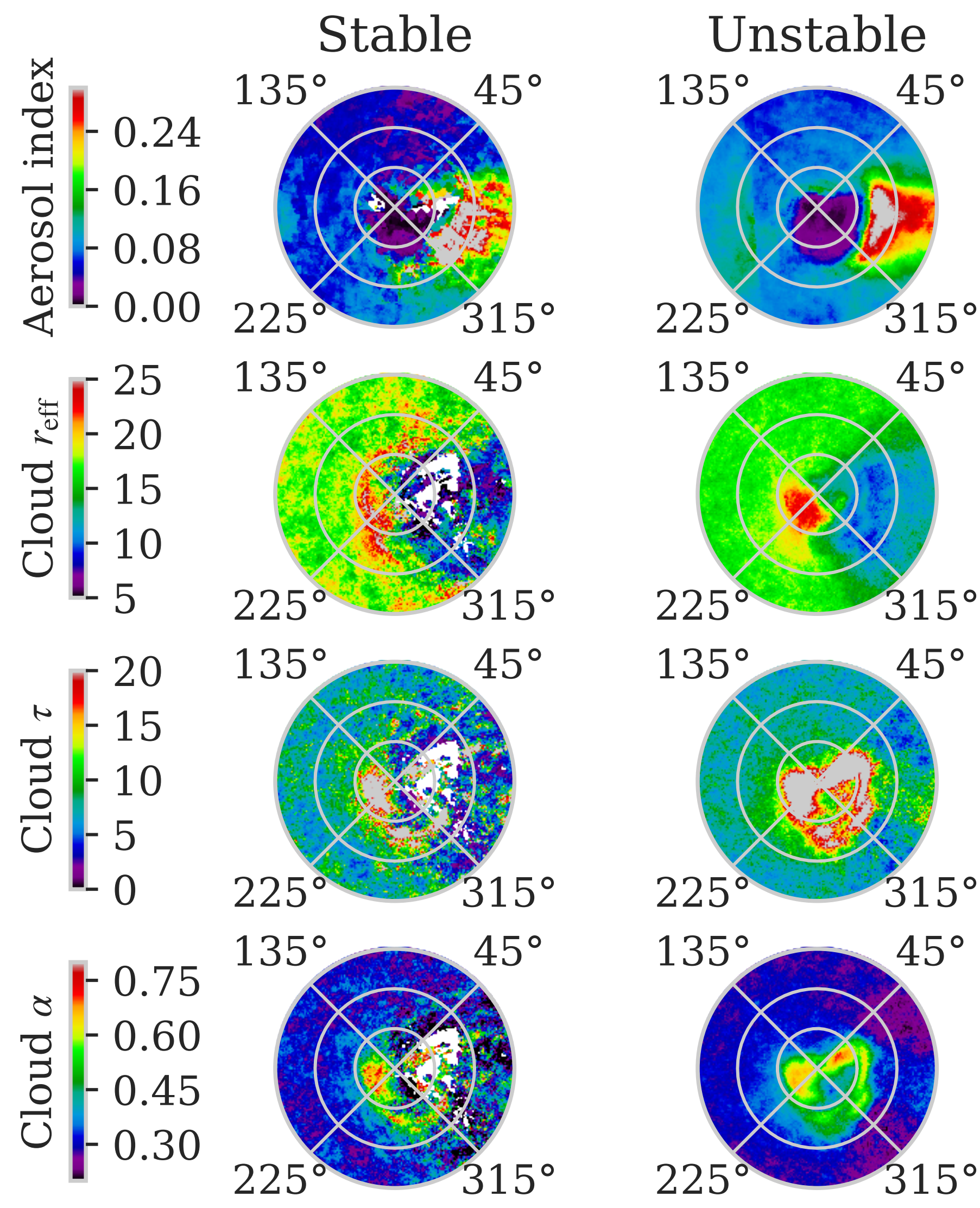


Following [6], if the downwind aerosol is dominated by these volcanic emissions, rotating the image into the direction of the wind (shown below, with the wind blowing from left to right) allows large volumes of data to be averaged. The result is aerosol and cloud properties as a function of distance and bearing from the source. For a remote site such as this, both clean and polluted conditions will be sampled, mapping cloud to aerosol properties.



There are many confounding variables, evident in the first figure from the enhanced aerosol optical depth (AOD) around cloud. To mitigate these effects, all aerosol retrievals within 7 km of a cloud has been excluded to avoid contamination [7] and pixels have been classified as wet/dry and un/stable based on the free tropospheric humidity and lower tropospheric stability reported by ERA-Interim. Averages were tabulated for aerosol and cloud optical depths and effective radii along with cloud albedo, cloud top height, and short and long-wave top-of-atmosphere fluxes.

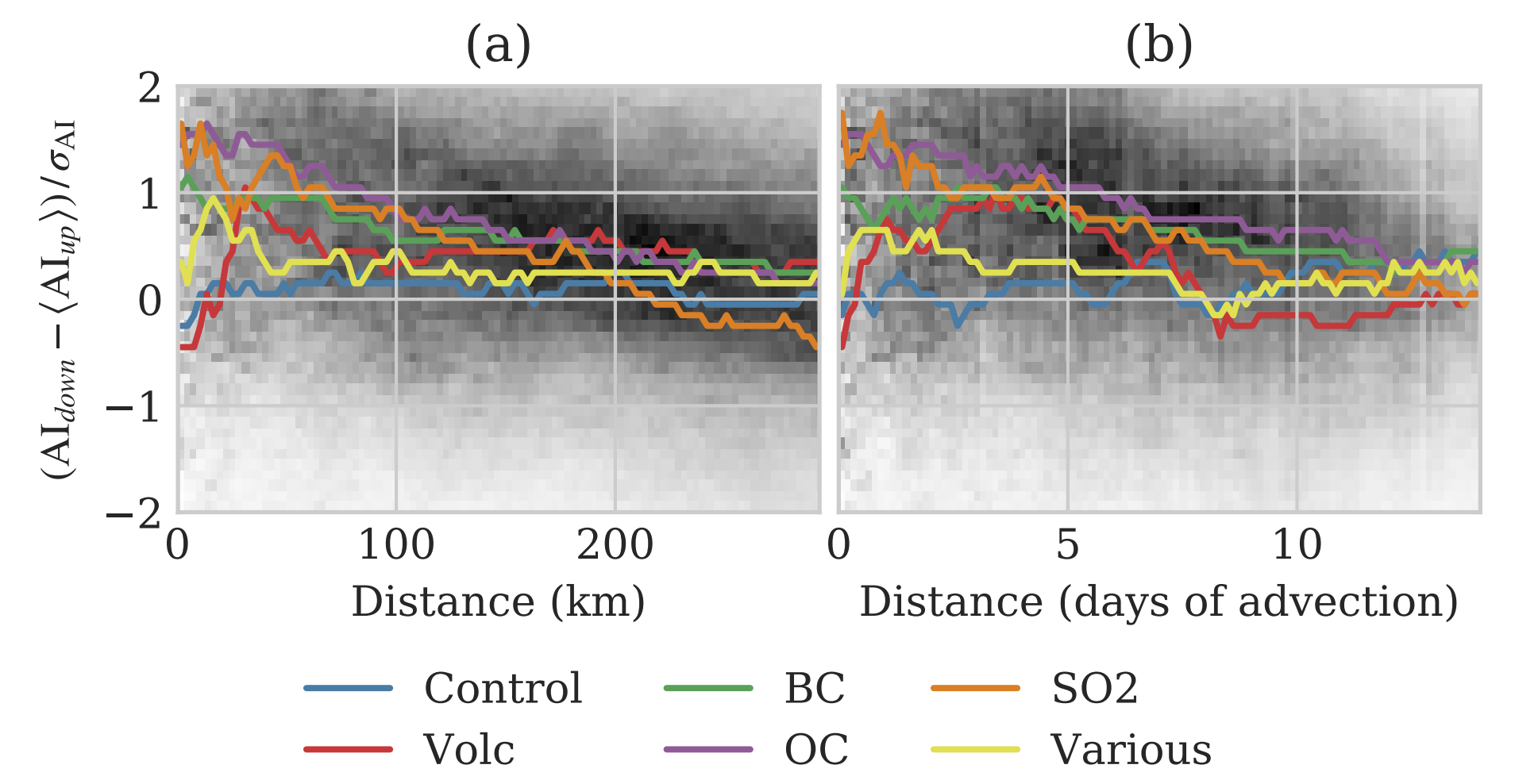
## Long-term averages



These show variation around Kilauea in 2002–2012 averages for stable and unstable humid atmospheres. While the aerosol is broadly similar, the cloud responds to both the presence of aerosol and the stability (note the narrow, downwind 'plume' in cloud albedo).

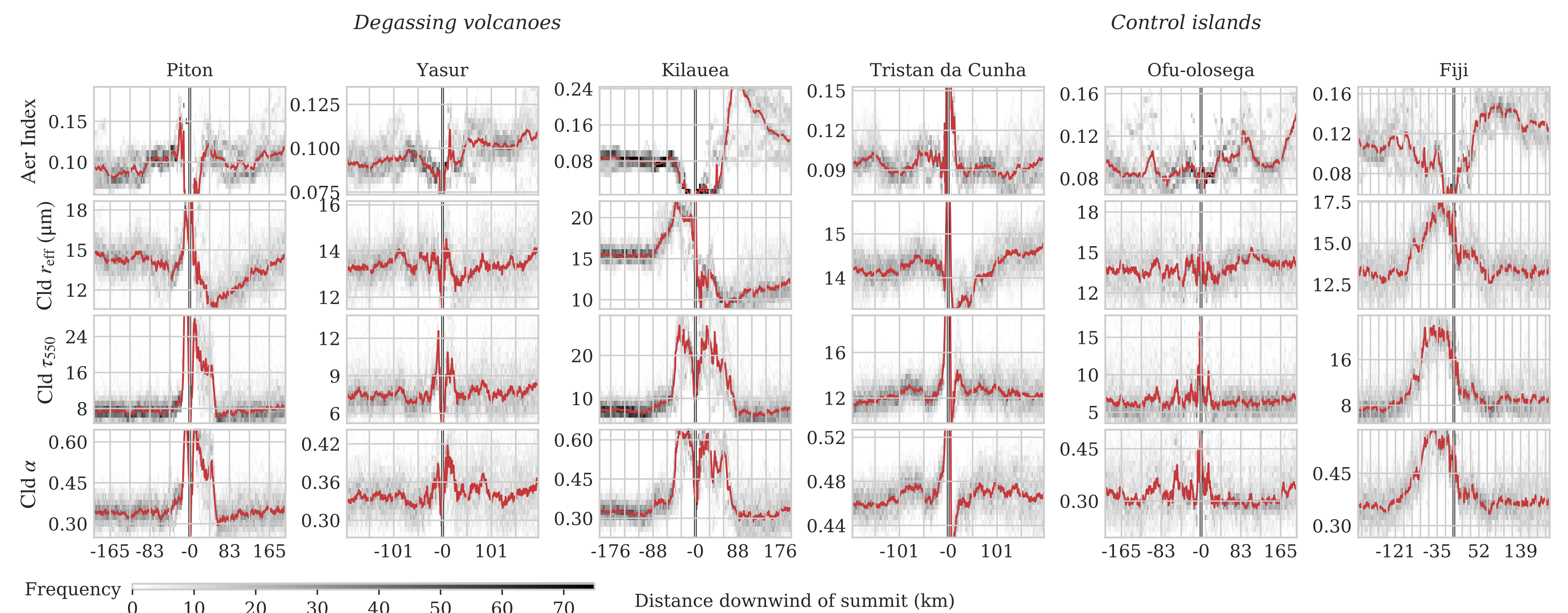
## Dominance of the sources

This technique was applied to 77 natural and anthropogenic aerosol sources alongside 11 controls, sampling a variety of aerosol types (shown opposite). Volcanoes were selected based on regular degassing. Frequent flaring was used to identify industrial areas. The CMIP6 inventory highlighted isolated areas of large or highly variable emissions. To assess the dominance of these sources, the plots below show the difference between aerosol index (AI) downwind and upwind of the source, normalised by its variability, as a function of (a) absolute distance from the source and (b) days of advection at the modal wind speed.

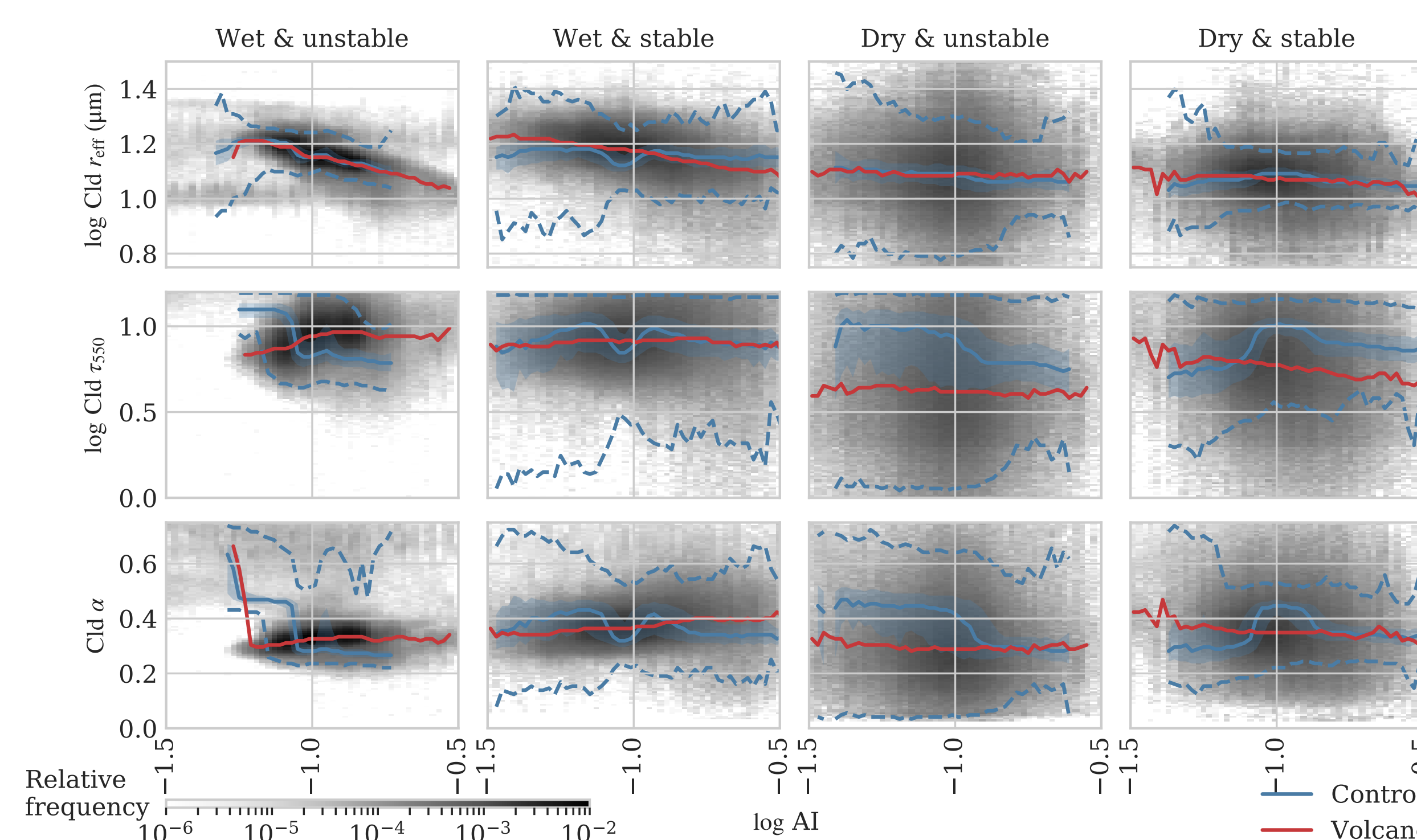


The controls and sites with no dominant aerosol type ('Various') show little change in aerosol enhancement with distance, indicating these sites are not dominant. Other classes affect the AI for about 200 km or 10 days.

## Retrievals before and after source compared to non-emitting islands

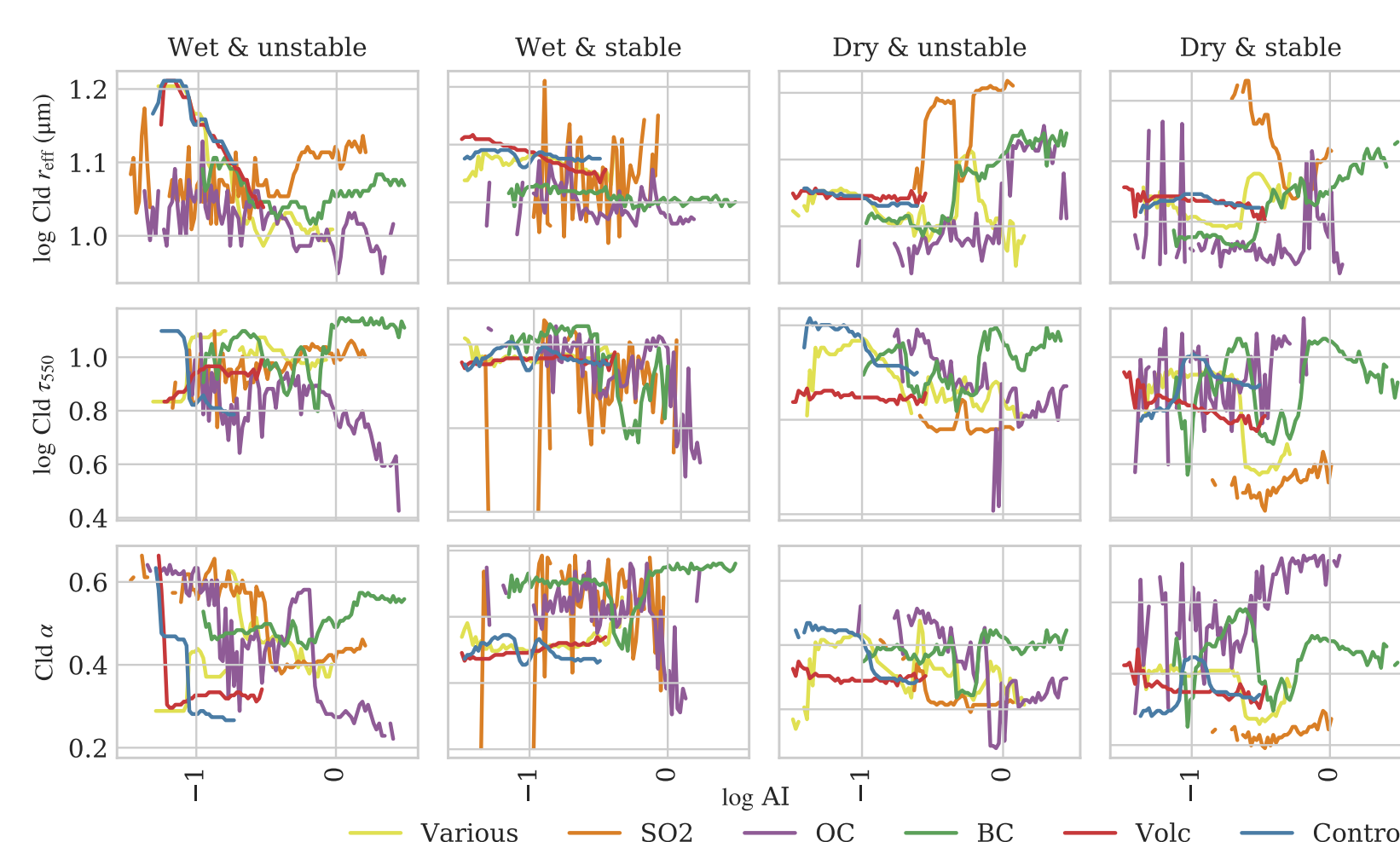


## Effective radius, optical depth, and albedo as functions of AI



The above plots show that the influence of volcanic aerosol on the cloud environment is more a shift in the edges of the distribution rather than a large-scale jump. The histograms opposite plot various cloud properties as a function of AI for each pixel around the 13 volcanoes studied (red: median, blue: median, quartiles, and percentiles of the control distribution). Changes in radius are evident in the controls and are stronger when moist, while an increase in albedo with AI is only seen for the perturbed clouds.

## Variation for different aerosol types



## Next steps and references

The data from anthropogenic sites needs better filtering. Ideally, the analysis would be repeated with more classes of humidity/stability to their local mean and would normalise distance by wind speed. A paper is in preparation for JGR.

- [1] T. Popp et al. (2016), doi:10.3390/rs8050421.
- [2] M. Stengel et al. (2017), doi:10.5194/essd-2017-48.
- [3] G.E. Thomas et al. (2009), doi:10.5194/amt-2-679-2009.
- [4] C.A. Poulsen et al. (2012), doi:10.5194/amt-5-1889-2012.
- [5] C. Rodgers (2000), Inverse Methods for Atmospheric Sounding: Theory and Practice, World Scientific.
- [6] S. Ebmeier et al. (2014), doi:10.5194/acp-14-10601-2014.
- [7] M.W. Christensen et al. (2017), doi:10.5194/acp-2017-450.